Ab Initio Investigation of the Diels–Alder Reaction between 2*H*-Phosphole and Phosphaethene: A Model for Phosphole Dimerization

ULRIKE SALZNER, STEVEN M. BACHRACH,* and DEBBIE C. MULHEARN

Department of Chemistry, Northern Illinois University, DeKalb, Illinois 60115

Received 16 January 1996; accepted 24 April 1996

ABSTRACT

All four possible Diels–Alder reactions between 2*H*-phosphole and phosphaethene were examined at various theoretical levels, including HF, MP4SDQ, CCSD(T), and CASSCF. MP2/6-31G* geometry optimizations could not be employed since the potential energy surface is qualitatively incorrect at this level of theory, due to the inherent underestimation of the activation energies (ameliorated at higher-order MP or coupled-cluster levels). Solvent effects were examined employing the Onsager, polarized continuum, and isodensity and surface polarized continuum models. At MP4SDQ/6-31G*//HF/6-31G* these reactions are exothermic by 34–38 kcal mol^{-1} and have very low activation energies, 5–7 kcal mol^{-1}. The P—P/C—C regioisomer products are lower in energy than the C—P isomers and, within each pair, the exo isomer is lower in energy. At low computational levels the smallest activation energy is for the reaction leading to the C—P endo product. Larger basis sets, electron correlation, and solvent favor the transition state leading to the experimentally observed P—P/C—P endo isomer. The dimerization of phosphole is, therefore, kinetically controlled. Based on geometric and electron density analysis, the reactions are concerted and synchronous.

Introduction

In 1982, Mathey *et al.*[1] reported the attempted synthesis of P-unsubstituted 1*H*-phospholes by protonation of 2,5-diphenyl- and 3,4-dimethylphospholyl anions. In contrast to the expected 1*H*-phospholes, they isolated the dimer **I** as a colorless solid. The composition of **I** was determined by elementary analysis, mass, and NMR spectroscopy. The presence of a P—P bond was confirmed by ^{31}P NMR spectroscopy. Crystal structure analysis[2] revealed that **I** has the endo struc-

* Author to whom all correspondence should be addressed.
E-mail: smb@smb.chem.niu.edu

CCC 0192-8651 / 97 / 020198-13

ture and that both the P—P and the C—C bonds connecting the two fragments are longer than ordinary P—P and C—C bonds. To explain the formation of **I**, Mathey proposed that the phospholyl anion is first protonated at phosphorus. The resulting 1*H*-phosphole rearranges to give 2*H*-phosphole, which then dimerizes by a [4 + 2] cycloaddition, one phosphole fragment acting as diene, the other as dienophile (Scheme I):

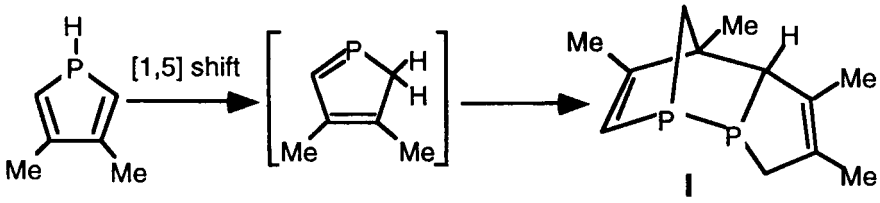

SCHEME I

The involvement of 2*H*-phospholes was further demonstrated by the synthesis of 1-phosphabicyclo[2.2.1]hepta-2,5-diene by reaction of 1*H*-phosphole with diphenylethyne.[3–5] Re-examination of the protonation of phospholyl anions[1,6] confirmed that, in the first step, 1*H*-phospholes are formed. 2*H*-phospholes could only be observed when complexed by $W(CO)_5THF$.[6] Later, Zurmühlen and Regitz were able to prepare a stable 2*H*-phosphole with bulky substituents.[7]

The reaction mechanism proposed by Mathey et al.[1] implies that: (a) the barrier for the 1,5-hydrogen shift in 1*H*-phosphole is sufficiently low to allow for rapid rearrangement; (b) the activation energy for 2*H*-phosphole dimerization is small, because 2*H*-phospholes cannot be isolated unless they are complexed or stabilized by bulky substituents; (c) 2*H*-phospholes are more reactive toward dimerization than the 1*H*-isomers, because no dimerization products of 1*H*-phospholes were observed; (d) dimerization of the 2*H*-phospholes are kinetically controlled, because the thermodynamically less stable endo isomer is obtained; and (e) the unexpected regioselectivity toward P—P/C—C bond formation must be either thermodynamically or kinetically more favorable than formation of two P—C bonds.

We have investigated the relative stabilities and activation energies for the rearrangement of phospholes.[8] These results fully support Mathey's interpretation of the experimental findings. At MP2/6-31G*, the barrier for the 1,5-hydrogen shift converting 1*H*-phosphole into 2*H*-phosphole is 16.2 kcal mol^{-1}. Moreover, the unsubstituted 2*H*-phosphole was found to be 5.63 kcal mol^{-1} lower in energy than 1*H*-phosphole. The relative energies of phosphole isomers, however, are reversed upon methyl or vinyl substitution.[9] Bachrach[10] further examined the reactivities of 1*H*-, 2*H*-, and 3*H*-phospholes in Diels–Alder reactions with acetylene. At MP4SDQ/6-31G*//MP2/6-31G*, the activation energy for the reaction involving 2*H*-phosphole is 18.50 kcal mol^{-1} lower than that for 1*H*-phosphole and 13.3 kcal mol^{-1} lower than that for 3*H*-phosphole.

The aim of the present study is to examine the stereo- and regioselectivity of the 2*H*-phosphole dimerization [with emphasis on implications (d) and (e) above]. Because calculation of phosphole dimerization is prohibitively expensive, we are modeling the 2*H*-phosphole dimerization by [4 + 2] cycloadditions between 2*H*-phosphole and phosphaethene. Reactants, products, and transition states for the four possible orientations of the dienophile relative to the diene (reactions 2–5) were located. The results are compared with those for the Diels–Alder reaction between 2*H*-phosphole and ethylene (reaction 1). Electronic structures of products and transition states are examined with topological electron density analyses.[11]

Theoretical Methods

The five reactions examined are drawn in Scheme II. All calculations were performed using GAUSSIAN 92[12a] or GAUSSIAN 94[12b]. Geometries were initially optimized at the HF/6-31G* level. Stability tests of the RHF/6-31G* wave functions of 2*H*-phosphole and for the transition states of reactions 2–5 revealed triplet instabilities. Therefore, we employed multireference (complete active

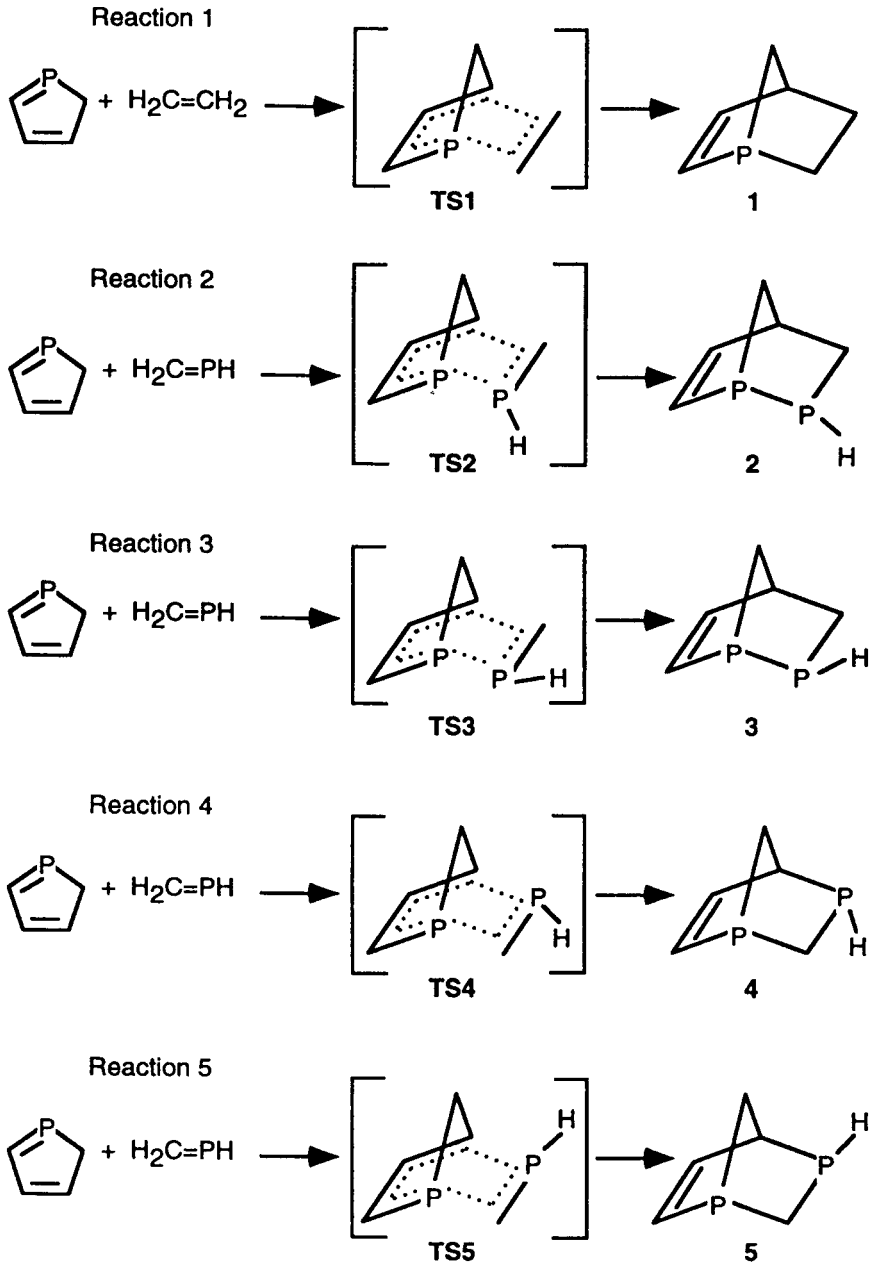

SCHEME II

space SCF–CASSCF) approaches in addition to single determinant (MP2–MP4 and coupled-cluster) methods. Geometry optimizations for educts and transition states were carried out at the RHF, MP2, and CASSCF levels and single point energies were computed at the MP4 and CCSD(T) levels using the 6-31G* basis set. For the CASSCF calculations, the π-orbitals and π-electrons were included in the active space, leading to a six-orbital–six-electron active space for the transition states. The effect of basis set enlargement was examined employing the Dunning 95* (D95*) basis set[13] at HF and MP2–MP4 levels. Solvent effects were included using the Onsager,[14–17] polarized continuum[18] (PCM), and isodensity surface polarized continuum[19] (IPCM) models at HF and MP2 with the 6-31G* and D95* basis sets. The reaction products were treated with single reference methods and the 6-31G* basis set only. Zero-point vibrational energy corrections were evaluated at the HF/6-31G* level and scaled by 0.89.[20]

The electron density of the HF wave functions was analyzed employing Bader's topological method.[11] Values of charge densities at bond criti-

cal points were evaluated using a locally modified version of EXTREME.[21] Bond orders are obtained from these charge densities using the empirical relationship, eq. (1), where $\rho(\mathbf{r}_c)$ is the value of the electron density at the bond critical point:

$$n(\mathrm{X—Y}) = \exp[\mathrm{A}[\,\rho(\mathbf{r}_c) - \mathrm{B}]] \qquad (1)$$

X—Y	A	B
C—P[22]	19.628	0.153
C—C[23]	6.458	0.252

Results

ENERGIES

Table I summarizes reaction and activation energies for reactions 1–5 at the MP4SDQ/6-31G*//HF/6-31G* + ZPE level of theory. All five reactions are strongly exothermic. Reactions 1, 4, and 5 have about the same exothermicity (around -34.3 kcal mol^{-1}). Reactions 2 and 3 (P—P and C—C bond formation), however, are more favorable: $\Delta E = -36.69$ (reaction 2) and -37.63 kcal mol^{-1} (reaction 3). Thus, P—P/C—C connected products **2** and **3** are thermodynamically favored over the C—P bonded isomers **4** and **5**. The exo products are thermodynamically favored over the endo products, but the energy differences are small: 0.94 kcal mol^{-1} for the P—P/C—C and 0.18 kcal mol^{-1} for the C—P products. Thus, in agreement with experiment,[1,2] the P—P bonded exoisomer is the thermodynamic product of the Diels–Alder reaction between 2*H*-phosphole and phosphaethene.

TABLE I.
Activation and Reaction Energies (kcal mol^{-1}) for Reactions 1–5 at Various Theoretical Levels Including Zero-Point Energy Correction (Basis Set is 6-31G* for All Cases).

Reaction		HF	MP2	MP3	MP4SDQ
1	ΔE	−31.11	−37.98	−35.51	−34.57
	E_a	*30.12*	*6.47*	*16.45*	*18.16*
2	ΔE	−37.33	−40.14	−37.96	−36.69
	E_a	*14.09*	*−5.03*	*3.96*	*5.80*
3	ΔE	−38.66	−40.99	−38.91	−37.63
	E_a	*15.83*	*−3.6*	*5.35*	*7.24*
4	ΔE	−34.77	−38.03	−35.10	−34.13
	E_a	*12.74*	*−5.81*	*2.72*	*4.65*
5	ΔE	−35.21	−38.04	−35.26	−34.31
	E_a	*14.97*	*−3.85*	*4.67*	*6.65*

At the MP4SDQ/6-31G*//HF/6-31G* + ZPE level, the activation energy for reaction 1 is 18.16 kcal mol^{-1}. This is quite similar to the barrier for the reaction of 2*H*-phosphole with ethyne (E_a = 17.9 kcal mol^{-1}).[10] Replacing one of the carbons in the ethene with phosphorus reduces the activation energy by 11–13 kcal mol^{-1}. Thus, the activation energies for reactions 2–5 are very low, 4.96–7.24 kcal mol^{-1}. This trend is consistent with previous results,[10,24] which showed that activation energies are lowered by about 10 kcal mol^{-1} compared to those of the parent systems when carbon is replaced by phosphorus in the diene fragment. The accuracy of the MP4/6-31G*//HF/6-31G* approach was examined for reaction 3 by evaluating the CCSD(T)/6-31G* energy employing the HF and MP2 geometries. The results are summarized in Table II. The CCSD(T) results indicate that the activation energy may actually be overestimated by around 2–3 kcal mol^{-1} at MP4SDQ.

Previous studies have shown that the activation energies of Diels–Alder reactions are significantly underestimated at MP2.[8,10,25] Because the activation energies for reactions 2–4 are so low at the HF level, *negative* values are obtained at MP2/6-31G*//HF/6-31G*. We reoptimized **TS5** at MP2/6-31G* and carried out an MP2 frequency calculation. The HF/6-31G* and MP2/6-31G* geometries of **TS5** differ only slightly and the MP2 structure is a true transition state with one imaginary frequency. Thus, an intermediate has to be present on the MP2/6-31G* surface. The intermediate lies 0.21 kcal mol^{-1} lower in energy than the transition state and 3.78 kcal mol^{-1} below the educts. The intermediate and transition state differ mainly in the P—C and C—P distances between the two fragments, which are longer in the intermediate by 0.38 and 0.36 Å, respectively. The potential energy surface is thus extremely flat in this region. No intermediate could be located at the RHF level. At MP4SDQ/6-31G*//MP2/631G* the transition state lies 2.91 kcal mol^{-1} above the educts and the intermediate is only 0.52 kcal mol^{-1} lower in energy than the educts. We could not locate a transition state between the intermediate and the educts. Thus, on the MP2 surface, the educts seem to convert without an energy barrier into the intermediate. For reaction 3, the MP2 optimized intermediate lies 0.10 kcal mol^{-1} lower in energy than the transition state and 3.27 kcal mol^{-1} below the educts. The P—P and C—P bond lengths are 0.34 and 0.30 Å longer in the intermediate than in the transition state. At MP4SDQ/6-31G*//MP2/6-31G* the transition state is 2.96

TABLE II.
Activation Energy (kcal mol^{-1}) for Reaction 3 at Various Theoretical Levels.

	Level[a]						
Geometry	HF	MP2	MP3	MP4SDQ	MP4SDTQ	CCSD	CCSD(T)
HF / 6-31G*	15.83	−3.60	5.35	7.24	1.32	7.30	3.82
MP2 / 6-31G*	10.97	−1.57	3.35	4.56	—	4.76	2.76

[a] The 6-31G* basis set is used for all calculations. Energies include the zero-point energy evaluated at HF / 6-31G*, which has been scaled by 0.89.

kcal mol^{-1} higher in energy than the educts and the intermediate lies 0.11 kcal mol^{-1} above the educts. For reactions 2 and 4, attempts to locate transition states and intermediates were unsuccessful at MP2. Thus, all four phosphole plus phosphaethene Diels–Alder reactions appear to proceed without a barrier at MP2/6-31G*. This is in contrast with higher level computations and with experiment which points to kinetically controlled formation of only one of four possible products. We believe that these data indicate that the MP2 potential energy surface is qualitatively incorrect due to the underestimation of activation energies for Diels–Alder reactions at this level of theory. Therefore, we will discuss only the HF/6-31G* geometries of the TSs.

The activation energies for reactions 2–5 (listed in Table I) indicate that there is a kinetic preference for *endo* over *exo* product formation. However, in disagreement with experiment the MP4SDQ/6-31G*//HF/6-31G* + ZPE data predict the C—P/C—P connected isomer to be kinetically favored. We therefore carried out several higher level computations to determine the relative energies of the four transition states more accurately. The results are summarized in Table III. At HF/6-31G* the activation energy for the formation of the C—P/C—P endo isomer is 1.35 kcal mol^{-1} lower than that for the P—P/C—C endo isomer. Extension of the basis set lowers this energy difference to 0.80 kcal mol^{-1}.

Inclusion of correlation has a similar effect. The CASSCF and MP4 relative energies are nearly identical, with **TS2** about 0.8 kcal mol^{-1} above **TS4**. Although the wave functions for the four transition states have significant multireference character, the similarity of the CASSCF/6-31G* and MP4 energies suggests that the multireference character of all four transition states is almost the same. Simultaneous improvement of basis set and correlation treatment further reduces the energy difference between C—P/C—P and P—P/C—C

TABLE III.
Relative Energies (kcal mol^{-1}) of Transition States TS2 – TS5 at Various Theoretical Levels.

	TS2	TS3	TS4	TS5
HF / 6-31G*	+1.35	+3.15	0.0	2.33
HF / D95*	+0.80	+2.61	0.0	+2.26
CASSCF(6,6) / 6-31G*	+0.78	+2.05	0.0	+1.69
MP2 / 6-31G* / / HF / 6-31G*	+0.78	+2.27	0.0	+2.07
MP3 / 6-31G* / / HF / 6-31G*	+1.24	+2.69	0.0	+2.06
MP4SDQ / 6-31G* / / HF / 6-31G*	+0.83	+2.33	0.0	+1.80
MP2 / D95G*	+0.04	+1.61	0.0	+1.91
MP4 / D95* / / HF / D95*	+0.53	+2.06	0.0	+1.97
HF / 6-31G* Onsager	+0.52	+2.28	0.0	2.34
HF / D95* Onsager	+0.30	+2.03	0.0	+2.28
HF / D95* PCM	+0.95	+2.72	0.0	
HF / D95* IPCM	+0.14	+1.71	0.0	+1.92
MP2 / D95* / / HF / D95* Onsager	0.0	+1.52	+0.46	+2.38
MP2 / D95* / / HF / D95* PCM	+0.28	+1.81	0.0	
MP2 / D95* / / HF / D95* PCM	0.0	+1.43	+0.28	+1.82
ZPE / HF / 6-31G*	0.0	−0.6	0.0	−0.11

transition states. At MP4/D95* the C—P/C—P transitions state is favored by 0.53 kcal mol^{-1}.

Since the dipole moments of the P—P/C—C are higher than those of the C—P/C—P transition states (3.1 vs. 1.4 D), we also examined solvent effects employing the Onsager,[14–17] polarized continuum[18] (PCM), and isodensity surface polarized continuum[19] (IPCM) models. A solvent with a dielectric constant of 50 has negligible influence on the geometry, but lowers the energies of the P—P/C—C relative to the C—P/C—P transition states by about 1 kcal mol^{-1}. Both the Onsager and IPCM calculations indicate that **TS4** is the lowest energy TS. The energy differences are small, so perhaps the safest conclusion is that **TS2** and **TS4** have similar energy when solvent effects are incorporated.

GEOMETRIES

The structures of the reaction products are given Figure 1. The only related experimentally determined structure is that of the 2*H*-phosphole dimer **I**.[2] Selected structural parameters for **I** and the corresponding adduct **2** at MP2/6-31G* are compared in Table IV. (While the MP2 method is inappropriate for optimization of the TSs, the MP2 surface is qualitatively correct in the region about the products. Since, in general, the MP2 geometries are more accurate than the HF geometries, we will discuss the MP2 geometries of the products. We note in passing that the HF/6-31G* geometries are not significantly different from the MP2 geometries reported here.) Because **I** and **2** differ in substitution and phase a perfect agreement is not to be expected. The overall correspondence, however, is quite reasonable. Table IV also lists MP2/6-31G* structural parameters for **1**, the exo P—P adduct **3**, and the endo and exo C—P adducts **4** and **5**.

There is little structural difference between **1** and the other norbornene products **2**–**5**. The two largest differences are: (1) the shorter C_4—C_5 distance in **1** (1.324 Å) than in **2**–**5** (about 1.35 Å); and (2) the angles about C_6 and C_7 are smaller than the corresponding angles in **2**–**5**.

Structures for the transition states of reactions 1–5 (at HF/6-31G*) are shown in Figure 2. Bond distances at HF/6-31G* and at CASSCF/6-31G* are summarized in Table V. HF/6-31G* data are

TABLE IV.
Comparison of Selected Structural Parameters of Mathey's 2H-Phosphole Dimer I with 1–5 at MP2/6-31G* (Bond Lengths Given in Angstroms and Bond Angles in Degrees).

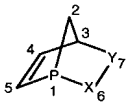

1: $X{=}Y{=}CH_2$
2, **3**: $X{=}PH$, $Y{=}CH_2$
4, **5**: $X{=}CH_2$, $Y{=}PH$

	I[a]	1	2	3	4	5
1–6	2.239(1)	1.887	2.260	2.243	1.898	1.893
3–7	1.577(5)	1.553	1.558	1.553	1.906	1.897
1–2	1.844(4)	1.864	1.872	1.870	1.865	1.861
1–5	1.812(4)	1.848	1.834	1.840	1.828	1.839
6–7	1.877(4)	1.552	1.882	1.889	1.872	1.878
2–3	1.542(5)	1.538	1.533	1.529	1.534	1.532
3–4	1.518(5)	1.517	1.500	1.506	1.493	1.500
4–5	1.337(5)	1.324	1.350	1.349	1.352	1.351
2–1–5	87.6(2)	87.5	87.2	87.2	87.6	87.2
2–1–6	86.0(1)	88.2	86.9	90.4	90.6	91.9
5–1–6	97.5(1)	94.5	95.7	91.0	96.0	94.6
1–6–7	93.3(1)	106.6	93.1	93.1	110.6	110.5
1–2–3	102.6(2)	97.5	101.4	101.3	101.0	101.0
2–3–7	104.2(3)	104.1	106.8	107.7	103.2	106.9
6–7–3	109.8(2)	106.9	109.4	109.0	92.7	92.7
3–7–11[b]	116.6(3)	109.4	109.2	110.4	97.2	97.2
1–6–13[b]	104.5(1)	109.9	95.8	95.8	97.2	96.3

[a] X-ray crystal structure from ref. 29.
[b] Atoms 11 and 13 are hydrogens, both in the endo position (**1**, **2**, and **4**) or exo position (**3** and **5**).

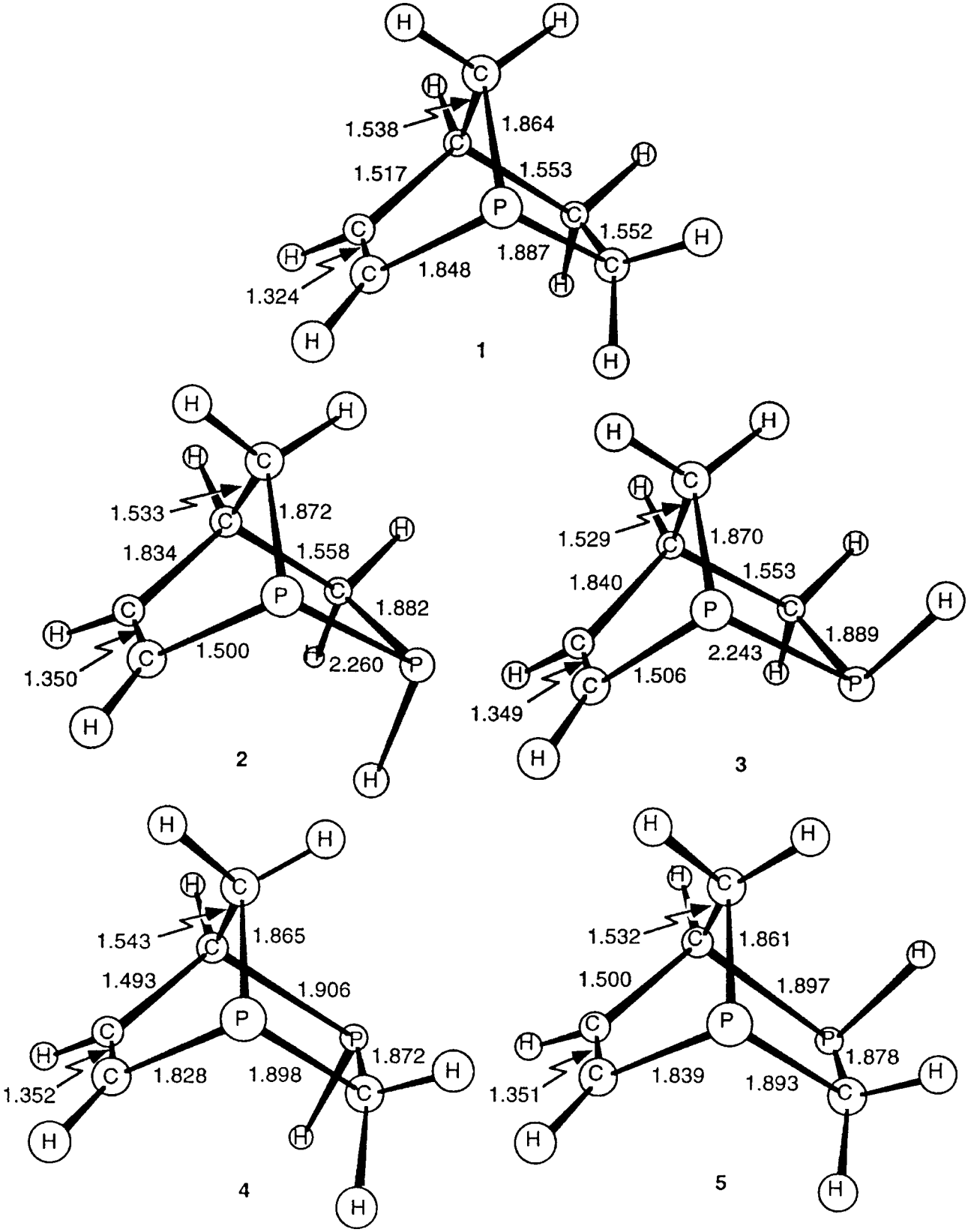

FIGURE 1. Geometries of **1**–**5** at MP2 / 6-31G*. All distances are in angstroms.

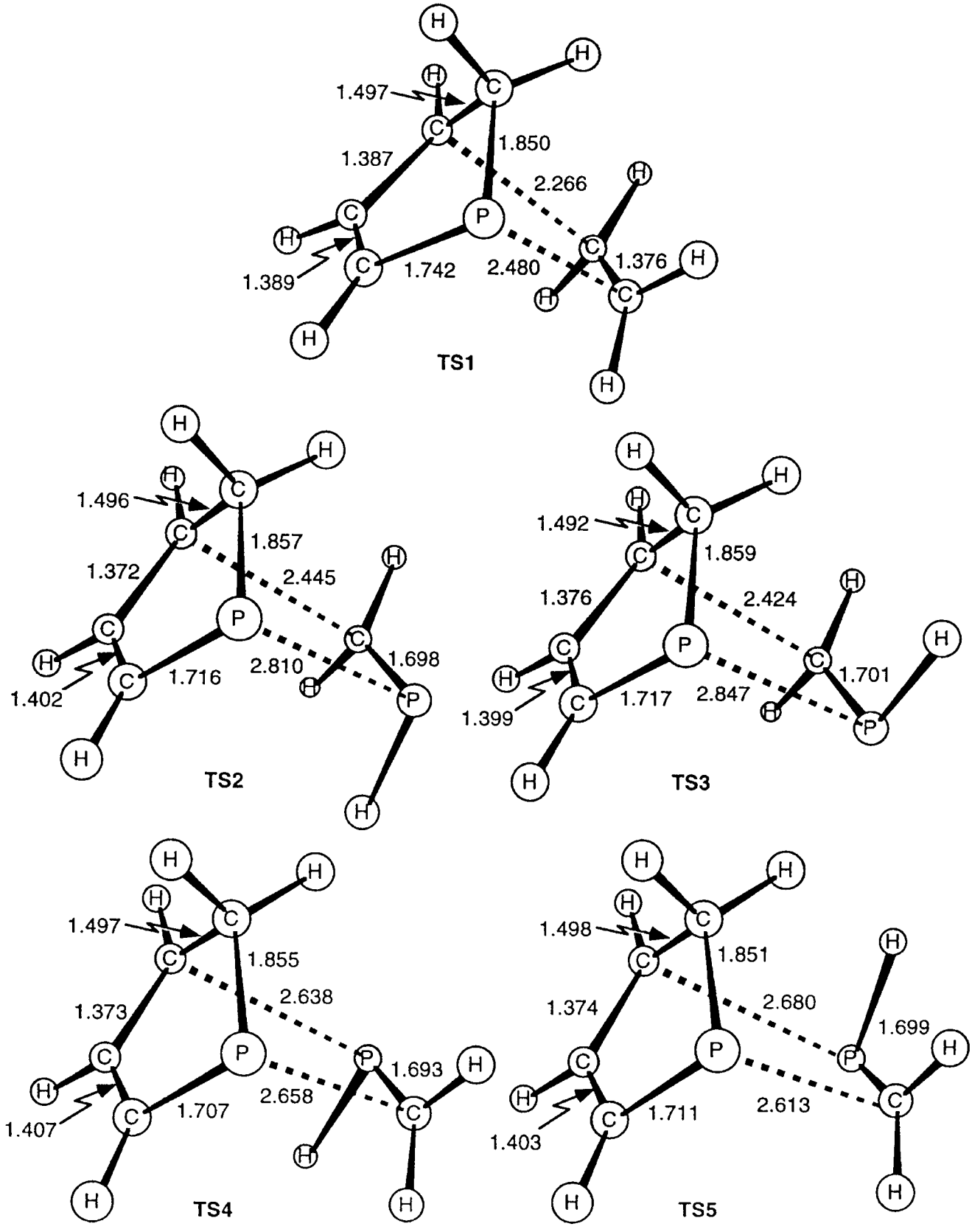

FIGURE 2. Geometries of **TS1**–**TS5** at HF / 6-31G*. All distances are in angstroms.

TABLE V.
Selected Geometrical Parameters[a] for TS1–TS5 at HF / 6-31G* and CASSCF(6,6) / 6-31G* (Bond Lengths Given in Angstroms and Bond Angles in Degrees).

	TS1	TS2		TS3		TS4		TS5	
	HF	HF	CAS	HF	CAS	HF	CAS	HF	CAS
1–6	2.480	2.810	2.780	2.847	2.813	2.658	2.606	2.613	2.576
3–7	2.266	2.445	2.449	2.424	2.441	2.638	2.664	2.680	2.715
1–5	1.724	1.716	1.744	1.717	1.746	1.707	1.737	1.711	1741
3–4	1.387	1.372	1.391	1.376	1.395	1.373	1.392	1.374	1.393
4–5	1.389	1.402	1.404	1.399	1.401	1.407	1.407	1.403	1.404
6–7	1.376	1.698	1.730	1.701	1.733	1.693	1.730	1.699	1.734
1–2	1.850	1.857	1.863	1.859	1.864	1.855	1.861	1.851	1.859
2–3	1.497	1.496	1.505	1.492	1.502	1.497	1.505	1.498	1.506
5–1–6	93.0	90.4	93.5	91.6	93.5	92.3	94.3	95.0	95.3
4–3–7	99.8	97.5	99.8	98.7	100.9	95.6	99.0	97.9	98.9
2–1–5	90.1	90.4	89.8	91.6	89.7	90.9	90.1	90.2	90.0
1–2–3	103.5	105.3	105.1	105.3	105.2	105.3	105.2	105.1	105.2
2–1–6	81.2	81.9	83.9	81.2	84.1	83.1	85.0	84.3	85.5
2–3–7	91.9	92.2	93.1	92.7	93.0	91.4	92.0	91.5	91.8
2–3–4	111.1	112.2	111.7	112.0	111.5	112.0	111.5	111.7	111.4

[a] For atom numbering, see Table IV.

compared to bond distances of infinitely separated educts in Table VI. As found by Li and Houk[26] for the parent Diels–Alder reaction, CASSCF and HF geometries are very similar. The distances between the phosphole phosphorus and the approaching phosphaalkenes are about 0.03 Å shorter in the CASSCF structures and the phosphole P—C double bonds are 0.03–0.05 Å longer. The forming bonds between the phosphole carbon and phosphaalkenes are 0.004–0.03 Å longer at CASSCF and the phosphole C—C double bonds lengthen by about 0.02 Å. The P—C double bonds in the alkene fragments are about 0.035 Å longer. The forming C—C double bonds in the phosphole fragments are unchanged. At both levels the geometries of the five TS are quite similar. The corresponding bond distances within the phosphole ring of each TS differ by no more than 0.017 Å, and if we examine just **TS2**–**TS5** the maximum variation is even smaller, only 0.010 Å at HF and still smaller at CASSCF. The P—C distance in the dienophile fragment of **TS2**–**TS5** varies by only 0.008 Å.

The forming bonds between the phosphole and the dienophile in the TSs have distances that fall in

TABLE VI.
Bond Lengths[a] Changes for TS1–TS5 with Respect to Infinitely Separated Educts at HF / 6-31G*.

	TS1	**TS2**	**TS3**	**TS4**	**TS5**
1–5	+0.052	+0.044	+0.045	+0.035	+0.039
3–4	+0.055	+0.040	+0.044	+0.041	+0.042
4–5	−0.070	−0.057	−0.060	−0.052	−0.056
6–7	+0.059	+0.046	+0.049	+0.041	+0.047
1–2	−0.019	−0.012	−0.010	−0.014	−0.018
2–3	+0.001	0.0	−0.004	+0.001	+0.002
2–1–5	−0.7	−0.4	+0.8	+0.1	−0.6
1–2–3	−3.2	−1.4	−1.4	−1.4	−1.6
2–3–4	−3.1	−2.0	−2.2	−2.2	−2.5

[a] For atom numbering, see Table IV.

small ranges: the C—C distance in the reactions that also form a P—P bond is about 2.44 Å, the C—P distance in the reactions that form two C—P bonds is about 2.59 Å, and the P—P distance is about 2.80 Å.

We note that bond length changes (relative to educts) in Table VI for **TS1** (2*H*-phosphole plus ethene) are larger than those for **TS2**–**TS5** (2*H*-phosphole plus phosphaethene).

ELECTRONIC STRUCTURES

Bond orders for the transition states of reactions 1–5 are given and compared to those in infinitely separated educts in Table VII. Because no empirical charge density–bond order parameters have been determined for P—P bonds, bond orders cannot be calculated for these bonds; bond critical points are nevertheless found for these bonds.

The bond orders indicate a concerted reaction. The bond orders in **TS2**–**TS5** are very similar. The bond orders in **TS1** differ from the rest in that they express greater change from reactants, that is, a later transition state.

Comparison of the bond orders in any one of the five TSs indicates that the bond changes are synchronous. The least synchronous case is **TS3**. Here, the P_6—C_7 bond order reduces by 0.40, while the other bonds lag only somewhat behind with changes of around 0.3. We have noted synchronous bond orders in other Diels–Alder transition states.[10,24] We also noted an apparent conservation of bond order in Diels–Alder TSs. For reactions 1, 4, and 5, the sum of the bond orders for the bonds directly involved in the reactions are 6.68, 6.79, and 6.72, respectively. Ideal bond order conservation would have a sum of seven.

Discussion

We first examine the geometries of the products, particularly to compare them with experiment. Mathey et al.[2] pointed out that the P—P and the C—C bonds connecting the two phosphole fragments of **I** are unusually long. The calculated P—P and C—C bond distances connecting the phosphole and phosphaethene fragments of **2** confirm this conclusion. The P—P distance is actually 0.02 Å longer than that in the crystal structure. Because our calculations refer to isolated and unsubstituted species in the gas phase, the long P—P distance is an intrinsic property of diphosphanorbornadiene **2** and is not due to crystal packing or steric repulsions in solid **I**. The calculated C—C bond is 0.02 Å shorter than that in the crystal but is still 0.02 Å longer than ordinary C—C distances. The same trend is apparent in **3**, **4**, and **5**. The C—P bonds in **4** and **5** are about 0.4–0.6 Å longer than ordinary C—P bonds. The bond distances in the endo isomers tend to be longer than those in the exo forms.

The calculated bond angles for **2** are within 1° of the experimental values with two exceptions: the 5–1–6 angle is 1.8° smaller and the 2–3–7 angle is 2.6° larger than those in crystalline **I**. This may be rationalized by the presence of the cyclopentadiene ring in the endo position in **I**, indicating that **I** suffers additional steric strain compared to the hydrogen substituted analog **2**. This is also obvious from a comparison of the 1–6–H13 and 3–7–H11 bond angles which are smaller than the corresponding bond angles in **I**.

The calculated C—P distances between the bridgehead phosphorus to the bridging carbon in

TABLE VII.
Bond Orders in TS1–TS4 Determined Using Eq. (1) and Differences with Corresponding Bond Orders in Infinitely Separated Educts for HF / 6-31G* Geometries and Wave Functions.

Bond[a]	TS1	Δ	TS2	Δ	TS3	Δ	TS4	Δ	TS5	Δ
1–6	0.05	*+0.05*					0.10	*+0.10*	0.08	*+0.08*
3–7	0.20	*+0.20*	0.25	*+0.25*	0.25	*+0.25*	0.10	*+0.10*	0.10	*+0.10*
1–5	1.58	*−0.29*	1.61	*−0.26*	1.61	*−0.26*	1.70	*−0.17*	1.67	*−0.20*
3–4	1.64	*−0.35*	1.73	*−0.26*	1.70	*−0.29*	1.72	*−0.27*	1.72	*−0.27*
4–5	1.57	*+0.33*	1.50	*+0.26*	1.52	*+0.28*	1.48	*+0.24*	1.50	*+0.26*
6–7	1.64	*−0.36*	1.63	*−0.37*	1.60	*−0.40*	1.69	*−0.31*	1.65	*−0.35*
1–2	1.06	*+0.09*	1.02	*+0.05*	1.01	*+0.04*	1.03	*+0.06*	1.05	*+0.08*
2–3	1.11	*0.0*	1.12	*+0.01*	1.13	*+0.02*	1.11	*0.0*	1.10	*−0.01*

[a] For atom numbering, see Table IV.

2–**5** are about 0.05 Å longer than normal. Such bond lengthening has been explained as an attempt to relieve strain.[10] We note, however, that the corresponding bond length in the crystal structure of **I** is that of an ordinary C—P single bond (1.844 Å). The calculated C—C bond distances between bridgehead and bridging positions in **2**–**5** are not lengthened compared to average C—C single bonds and are slightly shorter than those in the crystal.

In their review of pericyclic reactions, Houk et al.[27] noted that bond distances in these TSs fell within limited ranges; for example, the distance for the forming bond between two sp^2 carbon atoms is 1.90–2.28 Å. We noted that, in reactions that form new C—C and C—P bonds, such as the reaction of 1-phospha-1,3-butadiene with ethene,[24a] 1,3-butadiene with phosphaethene,[24b] and 2*H*-phosphole with ethyne,[10] the C—P distance in these TSs are typically in the range 2.55–2.59 Å. The forming C—P bond in **TS1** is 2.480 Å, suggesting a slightly larger range for these C—P distances. In **TS4** and **TS5**, the C—P distances are somewhat longer than this, ranging from 2.613 to 2.680 Å. Direct comparison between these two sets is not reasonable because two C—P bonds are being created in **TS4** and **TS5**, compared with one C—P and one (shorter) C—C bond in the previous work. Nevertheless, bond distances in these TSs do appear to fall in limited ranges.

To begin our discussion of the thermodynamics of our phosphole dimerization model, let us first compare the reaction energetics of similar Diels–Alder reactions. In our previous study,[10] we reported that for the reaction of cyclopentadiene with ethyne (MP4SDQ/6-31G* with ZPE corrections), the energy of reaction was -30.70 kcal mol^{-1} and the activation energy was 27.94 kcal mol^{-1}. Replacing a carbon in the ring with a phosphorus (the reaction of 2*H*-phosphole with ethyne) gives $\Delta E = -37.19$ kcal mol^{-1} and $E_a = 17.93$. Both reactions are very exothermic, but the phosphorus substitution leads to a dramatic decrease in the activation energy and reaction energy.

The source of the decrease in activation energy with phosphorus is breaking the weak C—P π-bond, recently estimated[28] as only 44 kcal mol^{-1}. This same effect is expected in comparing the reactions of 2*H*-phosphole with ethene vs. phosphaethene. The activation energy of reaction 1 is 18.16 kcal mol^{-1}, quite similar to the activation energy for the reaction of 2*H*-phosphole with ethyne. Replacement of one carbon in ethene with phosphorus (reactions 2–5) leads to a reduction in activation energy by 11–13 kcal mol^{-1}. Once again, the C—P π-bond is a very reactive site.

An alternative viewpoint is supplied by examining the frontier orbitals. Relative to cyclopentadiene, 2*H*-phosphole possesses a higher HOMO and a lower LUMO.[10,24a] According to FMO theory, this suggests that phosphole dimerization will have a lower activation energy than cyclopentadiene dimerization.

The dimers formed by creating the P—P linkage (**2** and **3**) are lower in energy than the alternative isomers (**4** and **5**) by more than 2 kcal mol^{-1}. While at first glance this may look unlikely, because the P—P bond is very weak, simple bond energy additivity actually favors the P—P isomers by about 5 kcal mol^{-1}. The weak P—P bond is offset by the strong C—C bond (83 kcal mol^{-1}), relative to the two C—P bonds (63 kcal mol^{-1}).[29] Mathey[30] has identified only the P—P isomers as products of the dimerization of phospholes. Our calculations indicate that the P—P regioisomers are more stable than the other options.

Simple FMO arguments also favor the formation of the P—P isomer. The maximum atomic orbital coefficient in both the HOMO and LUMO of 2*H*-phosphole is at phosphorus. The optimal overlap occurs, therefore, in the orientation that forms the P—P bond.

The activation energies for reactions 2–5 are small, ranging from 4.96 kcal mol^{-1} in reaction 4 to 7.24 kcal mol^{-1} in reaction 3. These very small activation energies rationalize the experimental difficulty[31] in isolating monomeric 2*H*-phosphole.

The isolated phosphole dimers all have endo stereochemistry,[30] however, heating the endo product results in the formation of the exo product.[31] We find the endo isomer **2** is almost 1 kcal mol^{-1} less stable than the exo isomer **3**. Further, the activation energy leading to the endo isomer is 1.39 kcal mol^{-1} (MP2/D95*//HF/D95* IPCM + ZPE) less than the activation energy leading to the exo isomer. The calculations support the experimental suggestion that the endo isomer **2** is kinetically favored over **3**, which is the thermodynamic product. Similarly, the exo isomer **5** is slightly more stable than the endo isomer **4**. The activation energy leading to the endo isomer **4** is 1.43 kcal mol^{-1} less than the barrier to the exo product. **5**

Mathey's experiments all produced the P—P/C—C endo isomer, which appears to be the kinetic product. While our calculations show a distinct preference for the endo isomer, low level calculations favor the C—P/C—P regioisomer. At HF/6-31G* **TS4** is 1.35 kcal mol^{-1} lower in energy than

TS2. Expansion of the basis set and inclusion of electron correlation reduces this difference to 0.53 kcal mol^{-1}, and all four TSs lie within 2 kcal mol^{-1}. The energy separation is very sensitive to the computational method with the increasing computational level favoring **TS2**, and the TS corresponding to the experimentally observed product.

Because the experiments are carried out in solution (usually THF), we determined the relative energies of the TSs using the Onsager and polarized continuum models. Using a dielectric constant of 50, at HF/6-31G* **TS4** is still favored over **TS2**, but only by 0.52 kcal mol^{-1}. At MP2/D95* with solvent corrections, **TS2** is the lowest energy TS. Unfortunately, due to computational restraints, we could not apply higher levels of electron correlation with the solvent corrections. Nevertheless, the trend is apparent—increasing basis set size, higher levels of electron correlation, and solvent effect all favor **TS2**. Thus, our calculations are consistent with Mathey's experiment: the dimerization of 2*H*-phosphole is kinetically controlled to produce the P—P/C—C endo isomer.

Last, we turn our attention to the question of the synchronicity of these reactions. These reactions are all concerted with some bond cleavage and formation having taken place in the TS. We have previously noted that the Diels–Alder reactions involving phosphaethene,[24b] phosphabutadienes,[24a] and phospholes[10] are remarkably synchronous.

Judging the degree of synchronicity is an inexact science, with two typical criteria used: bond lengths and bond orders. Using bond lengths is complicated by the inherent differences in bond lengths for bonds between different atoms. Thus, one can observe the very similar C_3—C_4, C_4—C_5, C_6—C_7, and bond lengths in **TS1** and conclude that there is little bond alternation, but how does one compare these with the P_1—C_5 length? Instead, one could use the bond length differences (see Table VI) between reactants and the TS. For **TS1**, we observe very similar bond length changes for these four bonds, which suggests a highly synchronous reaction, even with the presence of one phosphorus atom destroying the symmetry. In fact, the bond length changes in reactions 2–5 are all very similar, suggesting that these are synchronous as well. This method does not allow for comparisons of forming sigma bonds. For example, do the distances 2.480 Å for the C—P and 2.266 Å for C—C forming bonds in **TS1** indicate synchronicity?

Using bond orders, arrived in an empirical fashion, allows us to effectively examine different types of bonds. In this case, bond orders lead to the same conclusion as bond distances. The bond orders for the breaking/forming π-bonds in **TS2**–**TS5** vary only from 1.73 to 1.48, and the absolute value of the difference between these bond orders and the corresponding bonds in reactants are clustered at about 0.25. The bond order differences for the forming C_3—C_7 bonds in **TS2** and **TS3** are also 0.25. The other forming bonds lag somewhat behind this value, nevertheless, these reactions are synchronous.

The bond length and bond order changes in reaction 1 are larger than in the other reactions, suggesting a later transition state. This is consistent with the greater activation energy of reaction 1 compared to the other four reactions.

Conclusions

We have examined the Diels–Alder reactions between 2*H*-phosphole and phosphaethene as a model for the dimerization of 2*H*-phosphole. Formation of P—P/C—C and C—P/C—P connected products with endo or exo conformations proceed via a concerted and synchronous path. The reactions are exothermic and require activation energies of only 5–7 kcal mol^{-1}. This extreme kinetic instability of 2*H*-phosphole explains why direct observation of 2*H*-phospholes is difficult.

For the Diels–Alder reaction, substitution of a carbon with a phosphorus atom in the ring or in the dienophile leads to a systematic reduction of the activation energy of about 10 kcal mol^{-1}, due to the weak C—P π-bond.

The regioisomers having the P—P bond are lower in energy than the C—P isomers. For each pair of regioisomers, the exo isomer is lower in energy, but the TS leading to the endo isomer is lower in energy. The lowest activation energy we find is for production of the endo P—P isomer **2**; however, one must be sure to include electron correlation and solvent effects and extended basis sets. These *ab initio* results are consistent with simple FMO arguments which predict a lower activation barrier for phosphole dimerization relative to cyclopentadiene based on orbital energies, and also a preference for the P—P regioisomer based on orbital coefficients. Our results are in agreement with experiment, where only the P—P

isomer in its endo conformation is produced, which can be converted to the exo isomer upon heating.

Acknowledgments

The authors thank the donors of the Petroleum Research Fund, administered by the American Chemical Society, and the National Science Foundation, for generous support of this research. Some of the calculations reported here were performed at the National Center for Supercomputing Applications under Grant # CHE940001N and utilized the Cray Y-MP at the NCSA, University of Illinois at Urbana–Champaign.

References

1. G. de Lauzon, C. Charrier, H. Bonnard, and F. Mathey, *Tetrahed. Lett.*, **23**, 511 (1982).
2. G. de Lauzon, C. Charrier, H. Bonnard, F. Mathey, J. Fischer, and A. Mitschler, *J. Chem. Soc. Chem. Commun.*, 1272 (1982).
3. F. Mathey, F. Mercier, C. Charrier, J. Fischer, and A. Mitschler, *J. Am. Chem. Soc.*, **103**, 4595 (1981).
4. F. Mathey, *Acc. Chem. Res.*, **25**, 90 (1992).
5. P. le Goff, F. Mathey, and L. Ricard, *J. Org. Chem.*, **54**, 4754 (1989).
6. C. Charrier, H. Bonnard, G. de Lauzon, S. Holand, and F. Mathey, *Phosph. Sulf.*, **18**, 51 (1983).
7. F. Zurmühlen and M. Regitz, *J. Organomet. Chem.*, **332**, C1 (1987).
8. S. M. Bachrach, *J. Org. Chem.*, **58**, 5414 (1993).
9. S. M. Bachrach and L. M. Periott, *J. Org. Chem.*, **59**, 3394 (1994).
10. S. M. Bachrach, *J. Org. Chem.*, **59**, 5027 (1994).
11. R. F. W. Bader, *Atoms in Molecules—A Quantum Theory*, Oxford University Press, Oxford, UK, 1990.
12. (a) M. J. Frisch, G. W. Trucks, M. Head-Gordon, P. M. W. Gill, M. W. Wong, J. B. Foresman, B. G. Johnson, H. B. Schlegel, M. A. Robb, E. S. Replogle, R. Gomperts, J. L. Andres, K. Raghavachari, J. S. Binkley, C. Gonzalez, R. L. Martin, D. J. Fox, D. J. Defrees, J. Baker, J. J. P. Stewart, and J. A. Pople, Gaussian, Inc., Pittsburgh, PA, 1992; (b) M. J. Frisch, G. W. Trucks, H. B. Schlegel, P. M. W. Gill, B. G. Johnson, M. A. Robb, J. R. Cheeseman, T. Keith, G. A. Petersson, J. A. Montgomery, K. Raghavachari, M. A. Al-Laham, V. G. Zakrzewski, J. V. Ortiz, J. B. Foresman, J. Cioslowski, B. B. Stefanov, A. Nanayakkara, M. Challacombe, C. Y. Peng, P. Y. Ayala, W. Chen, M. W. Wong, J. L. Andres, E. S. Reploge, R. Gomperts, R. L. Martin, D. L. Fox, J. S. Binkley, D. J. Defrees, J. Baker, J. J. P. Stewart, M. Head-Gordon, C. Gonzales, and J. A. Pople, GAUSSIAN 94, Gaussian, Inc., Pittsburgh, PA, 1995.
13. T. H. Dunning and P. J. Hay, *Modern Theoretical Chemistry*, Plenum Press, New York, 1976, pp. 1–28.
14. M. W. Wong, K. B. Wiberg, and M. J. Frisch, *J. Am. Chem. Soc.*, **114**, 1645 (1992).
15. M. W. Wong, M. J. Frisch, and K. B. Wiberg, *J. Am. Chem. Soc.*, **113**, 4776 (1991).
16. M. W. Wong, K. B. Wiberg, and M. J. Frisch, *J. Chem. Phys.*, **95**, 8991 (1991).
17. M. W. Wong, K. B. Wiberg, and M. J. Frisch, *J. Am. Chem. Soc.*, **114**, 523 (1992).
18. (a) S. Miertus and J. Tomasi, *Chem. Phys.*, **65**, 239 (1982); (b) S. Miertus, E. Scrocco, and J. Tomasi, *Chem. Phys.*, **55**, 117 (1981).
19. M. J. Frisch, A. Frisch, and J. B. Foresman, *GAUSSIAN 94 User's Reference*, Gaussian, Inc., Pittsburgh, PA, 1994.
20. W. J. Hehre, L. Radom, P. v. R. Schleyer, and J. A. Pople, *Ab Initio Molecular Orbital Theory*, John Wiley & Sons, New York, 1986.
21. F. W. Biegler-Konig, R. F. W. Bader, and T. H. Tang, *J. Comput. Chem.*, **3**, 317 (1982).
22. S. M. Bachrach, *J. Mol. Struct.* (*Theochem*) **255**, 207 (1992).
23. T. S. Slee, In *Modern Models of Bonding and Delocalization*, J. F. Liebman and A. Greenberg, Eds., VCH Publishers, New York, 1988, p. 69.
24. (a) S. M. Bachrach and M. Liu, *J. Org. Chem.*, **57**, 6736 (1992); (b) S. M. Bachrach and D. C. Mulhearn, In *Proceedings of the First Electronic Computational Chemistry Conference —CD ROM*, S. M. Bachrach, D. B. Boyd, S. K. Gray, W. Hase, and H. S. Rzepa, Eds., ARInternet, Landover, MD, 1996.
25. (a) R. D. Bach, J. J. W. McDouall, and H. B. Schlegel, *J. Org. Chem.*, **54**, 2931 (1989); (b) K. N. Houk, R. J. Loncharich, J. F. Blake, and W. J. Jorgensen, *J. Am. Chem. Soc.*, **111**, 9172 (1989); (c) W. L. Jorgensen, D. Lim, and J. F. Blake, *J. Am. Chem. Soc.*, **115**, 2936 (1993).
26. Y. Li and K. N. Houk, *J. Am. Chem. Soc.*, **115**, 7478 (1993).
27. K. N. Houk, Y. Li, and J. D. Evanseck, *Angew. Chem. Int. Ed. Engl.*, **31**, 682 (1992).
28. K. B. Wiberg and D. Nakaji, *J. Am. Chem. Soc.*, **115**, 10658 (1993).
29. J. E. Huheey, E. A. Keiter, and R. L. Keiter, *Inorganic Chemistry*, 4th Ed., Harper Collins, New York, 1993.
30. F. Mathey, *Chem. Rev.*, **88**, 429 (1988).
31. C. Charrier, H. Bonnard, G. de Lauzon, and F. Mathey, *J. Am. Chem. Soc.*, **105**, 6871 (1983).